Laser and Particle Beams (2013), *31*, 187–193.

doi:10.1017/S0263034612001085

Effects of plasma and ultrashort laser pulse on residual electron energy in optical-field-ionized oxygen plasma

ESMAEIL ESLAMI AND KEYVAN BASEREH
Department of Physics, Iran University of Science & Technology, Narmak, Tehran, Iran
(RECEIVED 26 September 2012; ACCEPTED 12 November 2012)

Abstract

In this paper the classical theory of Above Threshold Ionization (ATI) in the oxygen plasma was used to show how the residual electron energy depends on the laser parameters such as pulse length, wavelength and peak intensity. The value of ATI energy is found to increase with laser wavelength and its intensity. Our study conducted for three cases of $\tau > 2\pi/\nu_p$, $\tau = 2\pi/\omega_p$, and $\tau < 2\pi/\omega_p$, where ω_p is the plasma frequency, reveals that the ATI energy is decreased for the pulse duration $\tau \neq 2\pi/\omega_p$. Also it is showed how the space charge effect can reduce the residual electron energy to a minimum value, in a suitable condition. By optimizing various parameters, we can generate the cold electrons suitable for the recombination x-ray laser.

Keywords: Above threshold ionization; Laser plasma interaction; Optical field ionization; X-ray laser

INTRODUCTION

Optical-field-ionization (OFI) X-ray laser driven by ultrashort high-power optical pulses has been considered as a promising candidate to provide high-repetition-rate, high-brightness, and coherent X-ray outputs (Corkum *et al.*, 1989; Ivanova, 2011; Lin, 2007; Mocek *et al.*, 2005; Morozov *et al.*, 2010; Sebban *et al.*, 2001). In this scheme, the electric field of laser pulse, interacts with the background gas or solid target, and produces plasma with partially or fully ionized ions along with free electrons (Bauer, 2003; Kuroda *et al.*, 2005). In this case, the atoms experience a sufficiently high electric field of an EM wave before the electron leaves the atom. This leads to the absorption of an integer number of photons in excess of the minimum photon number required for ionization. This process is called above-threshold ionization (ATI), which is mainly important at low densities where other heating mechanisms are ineffective (Becker *et al.*, 2002; Javanainen *et al.*, 1988). In reality, optical field intensity is high enough to modify the Coulomb potential of charge particles to create electrons by tunneling ionization (Augst *et al.*, 1989). This mechanism is very selective due to exponential dependence of the ionization rate on laser intensity and ionization potential.

Address correspondence and reprint requests to: Esmaeil Eslami, Department of Physics, Iran University of Science & Technology, Narmak, Tehran, 16846-13114, Iran. E-mail: eeslami@iust.ac.ir

Since the first soft X-ray laser was conclusively demonstrated in 1985 (Matthews *et al.*, 1985; Rosen *et al.*, 1985; Suckewer *et al.*, 1985), notable progress has been made in expanding the X-ray laser transition for applications in medicine, biology, chemistry, and physics. The first OFI X-ray laser was experimentally demonstrated in 1995 (Lemoff *et al.*, 1995). There are two general kinds of X-ray laser based on optical-field-induced ionization: One using a recombination scheme with hydrogen-like ions (Grout *et al.*, 1997; Nagata *et al.*, 1993; Yamaguchi *et al.*, 2002), and other using an electron collisional excitation scheme with non-hydrogen-like ions, where a very high degree of ionization is needed (Lemoff *et al.*, 1995; Ros *et al.*, 2002). In both cases, non-Maxwellian electron distributions may have a significant effect. The recombination compared to collisional excitation scheme requires relatively low pumping power. In this scheme, both the production of the cold electron, and a transition from an excited state to the ground state of ions, are suitable for making short-wavelength X-ray laser. As has been known for some years, plasmas generated by OFI with linearly polarized radiation are promising candidates for recombination X-ray-ultraviolet lasers because, in principle, extremely low electron temperatures can be achieved in relation to the ion stages produced (Rae & Burnett, 1992).

In laser plasma interaction, the laser mainly interacts with electrons, so the residual energy just after the irradiation of an ultrashort pulse laser, is given by the average energy of the

electrons in plasma. In fact, this energy is obtained from collisional heating (inverse Bremsstrahlung) and ATI energy. The collisional heating is significant for the long pulse (longer than the electron-electron and electron-ion collision time), where the substantial part of incident energy is consumed for heating the plasma via inverse Bremsstrahlung. In fact, at low density, ATI heating is dominant, while at high total densities inverse Bremsstrahlung heating begins to dominate since its heating rate is proportional to the ion density. In addition, Stimulated Raman scattering has become the most important parametric instability in laser-produced plasmas. This mechanism is also believed to be less effective in short pulse lasers (Eder *et al.*, 1992). Effect of ponderomotive force due to spatial inhomogeneisities in the laser field in ultrashort pulse, is returned to the wave and it does not contribute to ATI energy (Freeman *et al.*, 1987).

Many authors (Burnett & Corkum, 1989; Busuladžić *et al.*, 2009; Corkum, 1993; Corkum *et al.*, 1989; Paulus *et al.*, 1994) showed that if the electrons quiver energy is much greater than the photon energy and the ionization potential, the classical theory of ATI can be readily generalized to relativistic case. In reality, when the atoms absorb more photons than necessary for ionization, a series of peaks in the electron energy spectra appears. This phenomenon with various observed properties such as plateau and side lobes in the angular distribution may keep the ATI energy below the ionization potential. Thus, the ATI can be understood from classical consideration.

In this work, to obtain the ATI energy, we used a simple non-relativistic, non-quantum theoretical model for calculation of the electron energy in OFI oxygen plasma. The ATI energy is just the electron's energy long after the pulse has passed. In our calculation, the ions are kept immobile and move much more slowly than electrons. So their influence on the space charge field can be neglected. The sensitivity of the residual energy to the laser and plasma parameters such as electron and ions density, pulse duration, wavelength etc, in enhancing the residual energy will also be discussed.

TIME EVOLUTION OF THE ION DENSITY

A temporal Gaussian profile of the electric field of the laser pulse with frequency ω, intensity, I_0 (corresponding amplitude electric field E_0) and pulse duration τ is considered to propagate in a homogenous plasma of density n_p,

$$\vec{E}(r,t) = \vec{E}_0(r,t)\exp\left(-\frac{(t-t_m)^2}{\tau^2}\right). \quad (1)$$

Where t_m is the time corresponding to maximum intensity, and we consider a monochromatic linearly polarized light plan wave propagating along the z-axis with $\vec{E}_0(r,t) = E_0\cos(\omega t)\hat{x}$ and the peak electric field $E_0 = \sqrt{140\pi I}(V/cm)$. The intense electric field can ionize the neutral gas, and the numbers of electrons from the various charge states are created. If a stepwise production of multiply charge atomic ions is assumed, the evolution of ion density is given by a series of coupled equations, where the ground ion state plays the role of intermediate state. In this case, the rate equations take the form,

$$\frac{dn_j(t)}{dt} = \sum_{\substack{i=0\\ i<j}} W_{i,j}(t)n_i(t) - \sum_{k=j+1}^{Z_{max}} W_{j,k}(t)n_j(t) \quad (2)$$

Here $n_i(t)$, and $n_j(t)$ are the number density of species i, j at a specific time t, and $W_{ij}(t)$ is the ionization rate for production of a singly charged ion j from i. Z_{max} is the maximum produced charge state. The interaction of laser-plasma is governed by the Keldish parameter (Keldysh, 1964) in practical unit,

$$\gamma = \frac{2.31}{\lambda[\mu m]}\left(\frac{U_i[eV]}{I_0[TW/cm^2]}\right)^{1/2}. \quad (3)$$

Where U_i is the ionization potential of atom or ion with a charge state i, λ is the wavelength, and $I_0 \simeq (c\eta/8\pi)E_0^2$ is the average intensity of electromagnetic field in a rare field gas. There are many theoretical methods used to treat the ionization processes of atoms for $\gamma < 1$, such as Keldish (1964), barrier suppression ionization (Augst *et al.*, 1989; Penetrante & Bardsley, 1991), Amosov-Delone-Krainov (Ammosov *et al.*, 1989) theory, and so on. In the quasistatic or high-filed limit, $\gamma_k \ll 1$, from the general form of Keldish formula, the instantaneous ionization rate, $W(t)$, may be expressed as,

$$W(t) = 1.61\omega_{au}\frac{Z^2}{n_{eff}^{4.5}}\left(10.87\frac{Z^3}{n_{eff}^4}\frac{E_{au}}{E(t)}\right)^{2n_{eff}-1.5}\exp\left(-\frac{2}{3}\frac{Z^3}{n_{eff}^3}\frac{E_{au}}{E(t)}\right). \quad (4)$$

Where $\omega_{au} = 4.1\times10^{16}s^{-1}$ and $E_{au} = 5.1\times10^9 V/cm$ are the fundamental atomic frequency and field strength, respectively. $n_{eff} = Z/\sqrt{U_i[eV]/13.6}$ is the effective principal quantum number for a hydrogenic atom, where U_i in eV is the ionization potential, and Z is the charge of the produced ion. It is worth notice that the laser pulse duration is much shorter than the recombination time. In fact, the recombination rate for an electron of several ten of eV and electron density below 10^{20} cm^{-3} is on the order of nanosecond, so that during the pulse evolution, recombination terms in Eq. (2) could be neglected. The resulting set of ionization rate equations are stiff ordinary differential equations that may be solved routinely with standard initial value problem solvers (Byrne & Hindmarsh, 1987). Figure 1 shows the time evolution of the relative populations of the charge state oxygen ions for a pulse length $\tau = 100f_s$ ($t_{max} = 200f_s$) at wavelength ~ 532 nm for two different laser intensities; $I_0 = 10^{17}W/cm^2$ (1) and $I_0 = 10^{18}W/cm^2$ (2), respectively.

https://doi.org/10.1017/S0263034612001085 Published online by Cambridge University Press

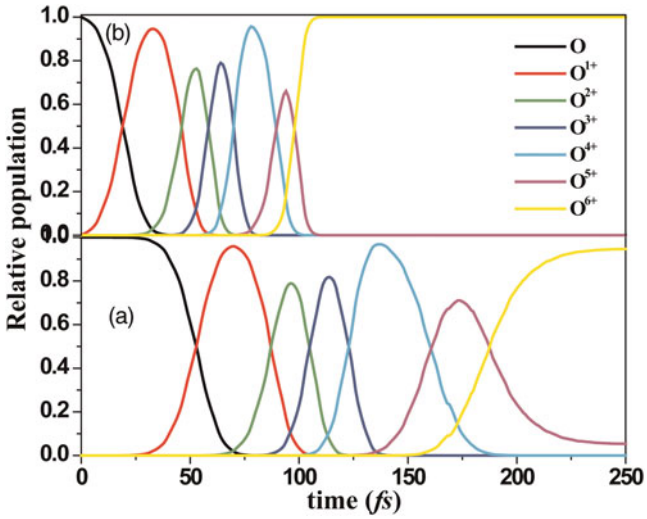

Fig. 1. (Color online) Time history of the average residual energy of electrons for the first six charge states of oxygen during laser pulse evolution for two different intensities $I_0 = 10^{17} W/cm^2$ (**a**) and $I_0 = 10^{18} W/cm^2$ (**b**), when pulse duration $\tau = 100\, fs$, and wavelength $\lambda = 532\, nm$.

The temporal variation of ionization population shows a step like behavior, because the electric field strength is sinusoidally oscillatory and the ionization rate depends strongly on the electric strength. Notice that the threshold laser intensity for OFI for hydrogenic ions is estimated by $I_{th} = 4 \times 10^9 U_i / Z^2 W/cm^2$ (Chichkov *et al.*, 1995). Each new ion states are created when the laser intensity reaches the level of threshold intensity. In our calculation, the highest charge state was O^{6+}. This is because the threshold intensity of the ions $\leq O^{6+}$ ($\sim 4 \times 10^{16}$ W/cm^2) (NIST) are significantly below the applied laser intensity. In addition, the lower ionization states ($< 2+$) are produced in the first half cycle of pulse. They are then rapidly vanished when the higher ionization states are generated. This means, the electrons can be created at different times over the laser pulse. In the highly ionized plasma, the electron motion can affect the pulse propagation in the plasma, and consequently, it can change the electron residual energy. These electrons account for the average ATI energy.

AVERAGE RESIDUAL ENERGY

The numbers of charged particles are produced from the various charge state at different time scale. They are thus subject to different accelerations, and the interactions among them are complicated. The electron velocity in the laser field is determined by the momentum equation,

$$\frac{d^2\vec{r}}{dt^2} = -\frac{e}{m_e}\vec{E}(t) + \vec{F}_{sch}(t). \tag{5}$$

Where $\vec{F}_{sch}(t) = -\omega_p^2 \vec{r}$ is the restoring force due to space charge effect, which can reduced the residual energy of electrons (Pulsifer *et al.*, 1994; Wilks *et al.*, 1995). e and m_e are the electron charge and mass relatively, and ω_p is the plasma frequency as a harmonic restoring force for the space-charge effect. In order to keep the residual energy small, the electron must interact with the EM field in nearly adiabatic fashion as laser pulse passes.

At the time of ionization, we assume that electrons have zero energy (Burnett & Corkum, 1989); therefore, they are classically accelerated by fields from the laser and from the surrounding plasma. Most of the electron energy during the laser pulse comes from the oscillatory quiver motion in the laser field, and is returned to the field when the pulse passed. In our calculation, the initial velocity of the ionized electron is taken to be zero at time t_0 at the origin r_0. t_0 is the time at which the electron is ionized by OFI process. If an electron is created at rest at this time in a linearly polarized laser pulse, it has a later time, t, with velocity,

$$\dot{x}(t_0, t) = \frac{eE_0}{m_e(\omega^2 - \omega_p^2)}[-\omega \sin(\omega t) + S_1(t_0)\cos(\omega_p t) + S_2(t_0)\sin(\omega_p t)]. \tag{6}$$

Where

$$S_1(t_0) = \left\{\omega \cos(\omega_p t_0)\sin(\omega t_0) - \omega_p \cos(\omega t_0)\sin(\omega_p t_0)\right\} \exp\left(-\frac{(t-t_m)^2}{\tau^2}\right),$$

$$S_2(t_0) = \left\{\omega \sin(\omega t_0)\sin(\omega_p t_0) + \omega_p \cos(\omega t_0)\cos(\omega_p t_0)\right\} \exp\left(-\frac{(t-t_m)^2}{\tau^2}\right). \tag{7}$$

The single electron kinetic energy after interaction with laser pulse over laser frequency, $2\pi/\omega$, is then given by,

$$\epsilon_{t_0} = \frac{<\dot{x}^2(t_0, t)>}{2m_e} = \epsilon_q + \epsilon_{ATI}(\omega, \omega_p, t_0). \tag{8}$$

Where $\epsilon_q = \frac{1}{4}\frac{e^2 E_0^2 \omega^2}{m_e(\omega^2 - \omega_p^2)^2}$. is the ponderomotive or quiver energy due to coherent oscillatory motion of electron, and the second term represents the excess energy of electron, and

https://doi.org/10.1017/S0263034612001085 Published online by Cambridge University Press

what has come to be known as the ATI energy.

$$\epsilon_{ATI}(\omega, \omega_p, t_0) = \frac{1}{4}\frac{e^2E_0^2}{m_e(\omega^2-\omega_p^2)^2}\left\{S_1(t_0)\left[1+\frac{\sin\left(\frac{4\pi\omega_p}{\omega}\right)}{\frac{4\pi\omega_p}{\omega}}\right]\right.$$
$$+S_2^2(t_0)\left[1-\frac{\sin\left(\frac{4\pi\omega_p}{\omega}\right)}{\frac{4\pi\omega_p}{\omega}}\right]-\frac{4}{\pi}S_1(t_0)\frac{\omega^3\sin\left(\frac{\pi\omega_p}{\omega}\right)}{\omega^2-\omega_p^2}$$
$$+\frac{2}{\pi}S_2(t_0)\frac{\omega^3\sin^2\left(\frac{2\pi\omega_p}{\omega}\right)}{\omega^2-\omega_p^2}$$
$$\left.+S_1(t_0)S_2(t_0)\frac{\sin^2\left(\frac{2\pi\omega_p}{\omega}\right)}{\frac{\pi\omega_p}{\omega}}\right\}. \quad (9)$$

Here we assumed the pulse length is much greater than an optical cycle time, $\tau_p \gg 2\pi/\omega$, and the electric field envelope is relatively constant. That is, ATI energy of each electron depends only on its own ionization time, t_0, when the electron becomes free of the atom. The average ATI or residual energy of all electrons by considering the number of electrons produced from the various charge states can be written,

$$\bar{\epsilon}_{ATI}(\omega, \omega_p) = \frac{\sum_{k=1}^{Z_{max}}\int_0^{t_{max}} n_k(t_0)W_k(t_0)\epsilon_{ATI}(\omega, \omega_p, t_0)dt_0}{\sum_{k=1}^{Z_{max}}\int_0^{t_{max}} n_k(t_0)W_k(t_0)dt_0}. \quad (10)$$

Where the integration is taken over the pulse envelope. It is obvious that the plasma containing higher ionization state would have a larger average ATI energy.

RESULTS AND DISCUSSION

Effect of Plasma Density on Residual Energy

Figure 2 shows the dependence of the residual energy as a function of plasma frequency normalized by laser frequency, ω_p/ω, for three different pulse intensities of 10^{16}, 10^{17}, and 10^{18} W/cm^2, respectively. Duration of linear polarized laser pulse is $\tau = 100$ fs at wavelength $\lambda = 532$ nm. The free electrons are coming from various charge state of oxygen. Clearly, the ATI energy gets larger with increasing laser intensity. If the density is so high that the effective plasma frequency ω_p approaches the laser frequency with increasing oxygen gas density, the resonance will occur; hence, the value of residual energy will become very large, as shown in figure. At electron densities close to the critical density, the plasma enhances the ATI energy by approximately a factor of 10. The non-uniform behavior of the curves is due to the modulation of the laser field amplitude. That is,

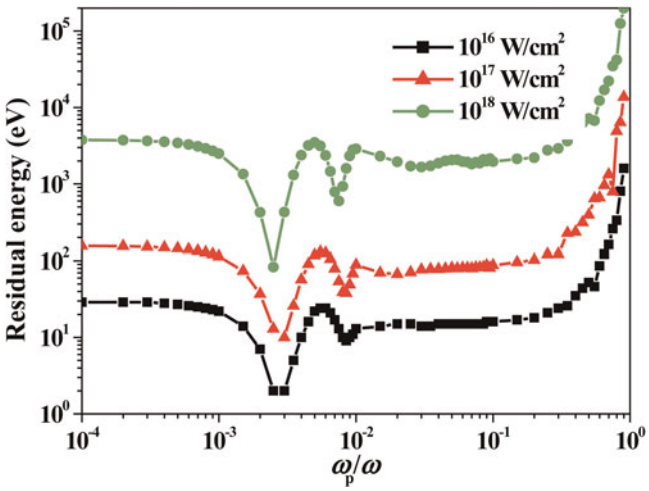

Fig. 2. (Color online) Dependence of average residual energy of electrons on plasma density ($\frac{\omega_p}{\omega}$) for three different laser pulse intensities $I_0 = 10^{16}W/cm^2$ (■), $I_0 = 10^{17}W/cm^2$ (▲) and $I_0 = 10^{18}W/cm^2$ (●), when pulse duration $\tau = 100\,fs$, and wavelength $\lambda = 532\,nm$.

large electron density corresponding to large plasma frequency produced effective electric field, which could alter the electric field of laser pulse. The fields then might cancel each other.

However, an enlarged part of the figure shows the ATI energy slightly decrease as the plasma density approaches $\omega_p/\omega \approx 10^{-3}$. This minimum in the residual energy is less dependent of the peak intensity and could simply achieve when $\omega_p \approx \pi/2\tau$ as shown in Figure 3 for two pulse durations $\tau = 500$ fs and $\tau = 500$ fs. However, the values of the electron residual energy in OFI plasmas are increased for the higher laser intensity as shown in Figure 2. Beyond this point and point for critical plasma density, it is found that low energy electrons with < 60 eV for the pulse length

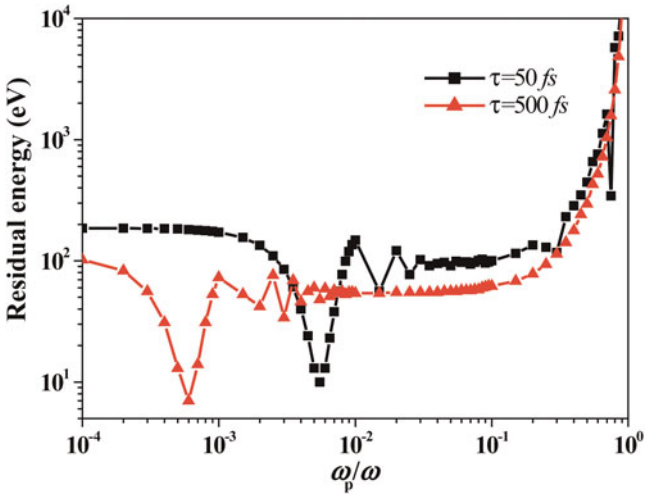

Fig. 3. (Color online) Dependence of average residual energy of electrons on plasma density ($\frac{\omega_p}{\omega}$) for two different pulse durations $\tau = 50\,fs$ (■), $\tau = 500\,fs$ (▲), when laser intensity $I_0 = 10^{17}W\ /\ cm^2$, and wavelength $\lambda = 532\,nm$.

https://doi.org/10.1017/S0263034612001085 Published online by Cambridge University Press

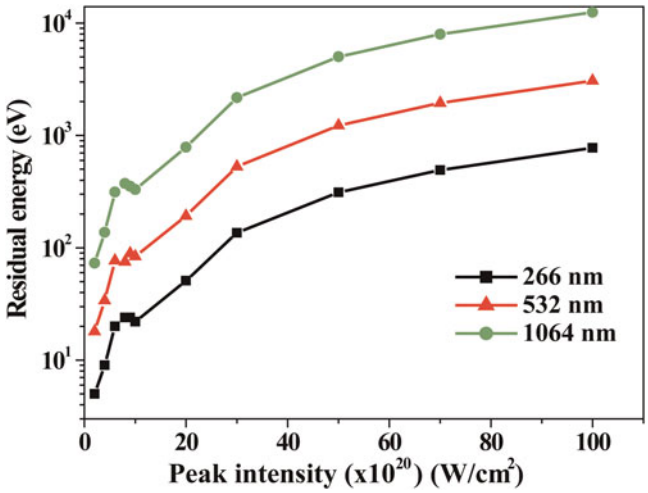

Fig. 4. (Color online) Variation of average residual energy of electrons with laser pulse intensity I_0 for three different light wavelength $\lambda = 266\ nm$ (■), $\lambda = 532\ nm$ (▲), and $\lambda = 1064\ nm$ (●) when pulse duration $\tau = 100\ fs$.

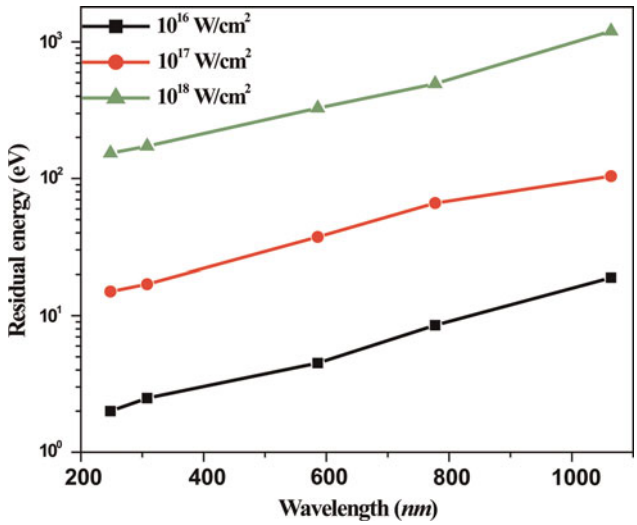

Fig. 5. (Color online) Variation of average residual energy of electrons with light wavelength for three different laser $I_0 = 10^{16} W/cm^2$ (■), $I_0 = 10^{17} W/cm^2$ (▲) and $I_0 = 10^{18} W/cm^2$ (●), when $\lambda = 532\ nm$, and pulse duration $\tau = 100\ fs$.

$\tau = 500$ fs can be produced in the density range of $10^{-4} < \omega_p/\omega < 10^{-1}$. Rapid recombination process to achieve high gain in X-ray plasma is more effective in the low electron temperature, and then the plasma density is chosen so that the ratio $\omega_p/\omega \approx 10^{-3}$ is valid for the rest of our analysis.

Effect of Laser Parameters on Residual Energy

The effect of laser intensity on average ATI energy of electrons in the three wavelengths, 266 nm, 532 nm, and 1064 nm, is shown in Figure 4, when the pulse duration is kept at 100 fs. The plasma frequency was about $\omega_p = 2.2 \times 10^{-3}\omega$, $\omega_p = 4.4 \times 10^{-3}\omega$, and $\omega_p = 6.6 \times 10^{-3}\omega$, respectively. It is clear from the figure that electron residual energy is larger with higher laser intensity. Further, a comparison between three wavelengths infers that largest energy is achieved for the longer wavelength.

Figure 5 shows the effects of laser frequency and the intensity for the same pulse duration as used in Figure 4. The ATI energy is found to vary with the square of laser wavelength, because the ionization rate of Eq. (4) is independent of the wavelength while the electron quiver energy depends on the square of the wavelength. However, the ATI energy are enhanced when wavelength is increased for all laser intensities. When we compare the slopes of the graphs in the figure, we notice that the average residual energy of electrons changes at a faster rate in the case of $I = 10^{18}$ W/cm^2. Therefore, the laser with higher intensity is found to be more sensitive with the wavelength. In the case of $I = 10^{16}$ W/cm^2, ATI energy at 266 nm is about one order of magnitude smaller than that at 1064 nm. However, similar to the last results, the residual energy are increased for the higher laser intensity. So, we can conclude that plasma with higher frequency is best suited for a cold electron production in the plasma. The decreased residual energy for larger frequency can be explained on the basis of velocity term in Eq. (6). Actually, the group velocity v_g gets larger with the increasing frequency. This leads to weaker driven force in the plasma as the frequency is appearing in denominator in Eq. (9). Therefore, the electrons with smaller ATI energy are created in the plasma. It is worth to notice that a laser operating with $I = 10^{16}$ W/cm^2, and $I = 10^{17}$ W/cm^2 at 226 nm, will produce electrons having an average energy of 2 eV, and 15 eV respectively, which are much smaller than an ionization potential of O^{2+} (35 eV), and O^{3+} (55 eV). These values, however, are not low enough to produce population inversion with respect to the ground state by rapid recombination. In Figure 6, we investigate the effect of laser pulse duration

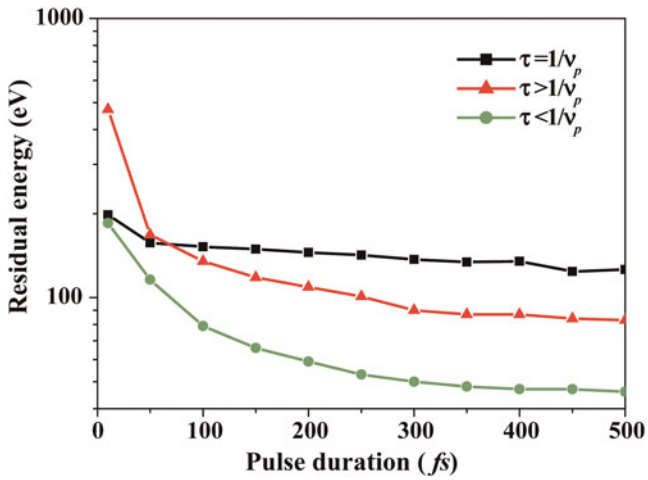

Fig. 6. (Color online) Variation of average residual energy of electrons with pulse duration τ for three different cases $\tau = 2\pi/\omega_p$ (■), $\tau > 2\pi/\omega_p$ (▲), and $\tau < 2\pi/\omega_p$ (●) when, $I_0 = 10^{17} W\ /\ cm^2$ and laser wavelength $\lambda = 532\ nm$.

https://doi.org/10.1017/S0263034612001085 Published online by Cambridge University Press

on the average ATI energy of electrons for three cases of $\tau = 2\pi/\omega_p$, $\tau > 2\pi/\omega_p$ and $\tau < 2\pi/\omega_p$ when $I = 10^{17} W/cm_2$ and $\lambda = 532nm$. From the figure it is evident that the laser pulse with $\tau \neq 2\pi/\omega_p$ is less effective for the high energy electron production in the plasma. The residual energy for all three cases goes down with increasing pulse duration. Therefore, it can be concluded that the narrow laser pulses are more suitable for the high electron energy production. A comparison between the three graphs shows that the ATI energy changes at a faster rate with the pulse duration when the plasma density and pulse duration satisfy the condition $\tau < 2\pi/\omega_p$. It means long pulses would generate low residual energy of the electrons to facilitate recombination and suppress collisional excitation. It is worth to notice that when we compare these results with ones in Figures 2 and 3, we find that there are two regions where the residual energy is relatively high. At the high-density where the plasma and laser frequency are close ($\omega \approx \omega_p$), and at the density where the plasma oscillation is approximately equal to laser pulse length ($\tau \approx 2\pi/\omega_p$). It means the pulses with $\tau \neq 2\pi/\omega_p$ would generate low ATI electron energy if used in the low density plasma.

Electron Energy Distribution Function

Although the collisional heating is significant in high density plasmas, but electron energy distributions are determined mainly by the ATI energy in low density plasmas. So adequate control of electron energy distribution is a critical issue for developing the OFI X-ray lasers. Figure 7 shows the residual electron energy distribution function for two different wavelengths, 532 nm, and 1064 nm for a laser intensity of $I = 10^{17} W/cm^2$, $\tau = 100fs$. ATI energy distribution of electrons produced by OFI from different ionization stages are obtained numerically by performing the summation indicated in the analytical form for the distribution function.

$$f_k(\epsilon_k)\Delta\epsilon = \sum_{k=1}^{Z_{max}} \sum_{t_0=0}^{t_{max}} n_t(t_0) W_i(t_0) \Delta t \tag{11}$$

Where $\epsilon_k = (\epsilon_{k+1} + \epsilon_k)/2$ and $\Delta\epsilon = (\epsilon_{k+1} - \epsilon_k)/2$.

For both case, the distribution function increases over the entire energy range as more and more electrons are released. It is evident that the calculated electron energy distribution is different from the Maxwellian distribution as reported by Mohideen *et al.* (1993). The electron distribution gets decrease exponentially at the energy between 0–0.1 KeV, and 0–1 KeV at wavelength 523 nm, and 1064 nm, respectively. At the high energy, the distribution rather slowly decreases for both cases.

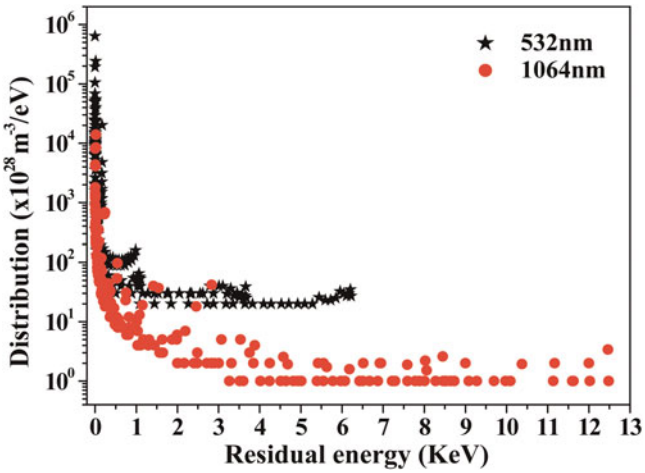

Fig. 7. (Color online) Electron energy distribution function versus ATI energy for two different wavelengths 532 *nm* (■), and 1064 *nm* (●). The laser conditions are $I_0 = 10^{17} W/cm^2$ and $\tau = 100\,fs$.

SUMMARY

In conclusion, a simple and effective approach to calculate the properties of OFI oxygen background gas has been presented. Numerical studies carried out in order to analyze the dependence of the ATI probabilities, as most important plasma heating mechanisms, on the laser field parameters (pulse duration, laser-field intensity, frequency), and background gas density. The presented results give indication that the laser-plasma parameters significantly alter the values of the electron residual temperature of the ionized neutrals in the plasma.

A careful investigation reveals that the effect of pulse duration could be stronger than that of the laser frequency on average ATI energy. In fact there are two regions where the residual energy is relatively high. At the high-density where the plasma and laser frequency are close ($\omega \approx \omega_p$). At the density where the plasma oscillation is approximately equal to laser pulse length ($\tau \approx 1/v_p$). Based on our numerical studied we observed that slower electrons can be generated under the situation of pulse duration much smaller than the plasma period and lower wavelengths. In each case, higher intensity pulses produce higher ATI electron energy.

Therefore, a judicious choice of laser pulse parameters and the plasma density can lead to cold electrons for the effective role in realizing a recombination pumping X-ray laser in an OFI plasma (Burnett & Enright, 1990; Hulin *et al.*, 2000).

ACKNOWLEDGEMENT

This work was partly supported by the IUST grant no 160/1226.

REFERENCES

Ammosov, M.V., Delone, N.B. & Krainov, V.P. (1989). Tunnel ionization of complex atoms and of atomic ions in an alternating electromagnetic field. *J.Exper. Theor. Phys.* **64**, 4.

https://doi.org/10.1017/S0263034612001085 Published online by Cambridge University Press

Augst, S., Strickland, D., Meyerhofer, D.D., Chin, S.L. & Eberly, J.H. (1989). Tunneling ionization of noble gases in a high-intensity laser field. *Phys. Rev. Lett.* **63**, 2212–2215.

Bauer, D. (2003). Plasma formation through field ionization in intense laser-matter interaction. *Laser Part. Beams* **21**, 489–495.

Becker, W., Grasbon, F., Kopold, R., Milošević, D.B., Paulus, G.G. & Walther, H. (2002). Above-threshold ionization: From classical features to quantum effects. *Advan. Atom., Molecul. Opt. Phys. B* **48**, 35–98.

Burnett, N.H. & Corkum, P.B. (1989). Cold-plasma production for recombination extremeultraviolet lasers by optical-field-induced ionization. *J. Opt. Soc. Am. B* **6**, 1195–1199.

Burnett, N.H. & Enright, G.D. (1990). Population inversion in the recombination of optically-ionized plasmas. *Quan. Electr., IEEE J.* **26**, 1797–1808.

Busuladžić, M., Gazibegović-Busuladžić, A. & Milošević, D.B. (2009). Strong-field approximation for ionization of a diatomic molecule by a strong laser field. III. High-order above-threshold ionization by an elliptically polarized field. *Phys. Rev. A* **80**, 013420.

Byrne, G.D. & Hindmarsh, A.C. (1987). Review of current and coming attractions. *J Comput. Phys.* **70**, 1–62.

Chichkov, B.N., Egbert, A., Eichmann, H., Momma, C., Nolte, S. & Wellegehausen, B. (1995). Soft-X-ray lasing to the ground states in low-charged oxygen ions. *Phys. Rev. A* **52**, 1629–1639.

Corkum, P.B. (1993). Plasma perspective on strong field multiphoton ionization. *Phys. Rev. Lett.* **71**, 1994–1997.

Corkum, P.B., Burnett, N.H. & Brunel, F. (1989). Above-threshold ionization in the long-wavelength limit. *Phys. Rev. Lett.* **62**, 1259–1262.

Eder, D.C., Amendt, P. & Wilks, S.C. (1992). Optical-field-ionized plasma X-ray lasers. *Phys. Rev. A* **45**, 6761–6772.

Freeman, R.R., Bucksbaum, P.H., Milchberg, H., Darack, S., Schumacher, D. & Geusic, M.E. (1987). Above-threshold ionization with subpicosecond laser pulses. *Phys. Rev. Lett.* **59**, 1092–1095.

Grout, M.J., Janulewicz, K.A., Healy, S.B. & Pert, G.J. (1997). Optical-field induced gas mixture breakdown for recombination X-ray lasers. *Opt. Commun.* **141**, 213–220.

Hulin, S., Auguste, T., D'Oliveira, P., Monot, P., Jacquemot, S., Bonnet, L. & Lefebvre, E. (2000). Soft-X-ray laser scheme in a plasma created by optical-field-induced ionization of nitrogen. *Phys. Rev. E* **61**, 5693–5700.

Ivanova, E.P. (2011). Highly efficient tabletop X-ray laser at $\lambda =$ 41.8 nm in Pd-like xenon pumped by optical-field ionization in a cluster jet. *Phys. Rev. A* **84**, 043829.

Javanainen, J., Eberly, J.H. & Su, Q. (1988). Numerical simulations of multiphoton ionization and above-threshold electron spectra. *Phys. Rev. A* **38**, 3430–3446.

Keldysh, L.V. (1964). Ionization in the field of a strong electromagnetic wave. *Zh Eksperim i Teor Fiz* **47**, 1945–1957.

Kuroda, H., Suzuki, M., Ganeev, R., Zhang, J., Baba, M., Ozaki, T. & Wei, Z.Y. (2005). Advanced 20 TW Ti: S laser system for X-ray laser and coherent XUV generation irradiated by ultrahigh intensities. *Laser Part. Beams* **23**, 396–396.

Lemoff, B.E., Yin, G.Y., Gordon Iii, C.L., Barty, C.P.J. & Harris, S.E. (1995). Demonstration of a 10-Hz femtosecond-pulse-driven XUV laser at 41.8 nm in Xe IX. *Phys. Rev. Lett.* **74**, 1574–1577.

Lin, J.Y. (2007). Optimization of laser propagation in optical-field-ionization plasmas for X-ray laser generation. *Appl. Phys. B* **86**, 25–29.

Matthews, D.L., Hagelstein, P.L., Rosen, M.D., Eckart, M.J., Ceglio, N.M., Hazi, A.U., Medecki, H., MacGowan, B.J., Trebes, J.E., Whitten, B.L., et al. (1985). Demonstration of a Soft X-Ray Amplifier. *Phys. Rev. Lett.* **54**, 110–113.

Mocek, T., Sebban, S., Bettaibi, I., Zeitoun, P., Faivre, G., Cros, B., Maynard, G., Butler, A., McKenna, C. & Spence, D. (2005). Progress in optical-field-ionization soft X-ray lasers at LOA. *Laser Part. Beams* **23**, 351–356.

Mohideen, U., Sher, M.H., Tom, H.W.K., Aumiller, G.D., Wood II., O.R., Freeman, R.R., Boker, J. & Bucksbaum, P.H. (1993). High intensity above-threshold ionization of He. *Phys. Rev. Lett.* **71**, 509–512.

Morozov, A., Luo, Y., Suckewer, S., Gordon, D. & Sprangle, P. (2010). Propagation of ultrashort laser pulses in optically ionized gases. *Phys. Plasmas* **17**, 023101.

Nagata, Y., Midorikawa, K., Kubodera, S., Obara, M., Tashiro, H. & Toyoda, K. (1993). Soft-X-ray amplification of the Lyman-α transition by optical-field-induced ionization. *Phys. Rev. Lett.* **71**, 3774–3777.

Paulus, G.G., Becker, W., Nicklich, W. & Walther, H. (1994). Rescattering effects in above-threshold ionization: a classical model. *J. Phys. B: Atom., Molecul. Opt. Phys.* **27**, L703.

Penetrante, B.M. & Bardsley, J.N. (1991). Residual energy in plasmas produced by intense subpicosecond lasers. *Phys. Rev. A* **43**, 3100–3113.

Pulsifer, P., Apruzese, J.P., Davis, J. & Kepple, P. (1994). Residual energy and its effect on gain in a Lyman-α laser. *Phys. Rev. A* **49**, 3958–3965.

Rae, S.C. & Burnett, K. (1992). Possible production of cold plasmas through optical-field-induced ionization. *Phys. Rev. A* **46**, 2077–2083.

Ros, D., Jamelot, G., Carillon, A., Jaegle, P., Klisnick, A., Zeitoun, P., Rus, B., Joyeux, D., Phalippou, D. & Boussoukaya, M. (2002). State of the development of X-ray lasers and applications at LSAI. *Laser Part. Beams* **20**, 23–30.

Rosen, M.D., Hagelstein, P.L., Matthews, D.L., Campbell, E.M., Hazi, A.U., Whitten, B.L., MacGowan, B., Turner, R.E., Lee, R.W., Charatis, G., et al. (1985). Exploding-foil technique for achieving a soft X-ray laser. *Phys. Rev. Lett.* **54**, 106–109.

Sebban, S., Haroutunian, R., Balcou, P., Grillon, G., Rousse, A., Kazamias, S., Marin, T., Rousseau, J.P., Notebaert, L., Pittman, M., et al. (2001). Saturated Amplification of a Collisionally pumped optical-field-ionization soft X-ray laser at 41.8 nm. *Phys. Rev. Lett.* **86**, 3004–3007.

Suckewer, S., Skinner, C.H., Milchberg, H., Keane, C. & Voorhees, D. (1985). Amplification of stimulated soft X-ray emission in a confined plasma column. *Phys. Rev. Lett.* **55**, 1753–1756.

Wilks, S., Kruer, W., Williams, E., Amendt, P. & Eder, D. (1995). Stimulated Raman backscatter in ultraintense, short pulse laser–-plasma interactions. *Phys. Plasmas* **2**, 274.

Yamaguchi, N., Fujikawa, C., Okasaka, K. & Hara, T. (2002). Production of highly ionized plasma by micro-dot array irradiation and its application to compact X-ray lasers. *Laser Part. Beams* **20**, 73–77.